

Bipedal Robot Running: Human-like Actuation Timing Using Fast and Slow Adaptations

Yusuke Sakurai¹, Tomoya Kamimura¹, Yuki Sakamoto¹, Shohei Nishii¹,
Kodai Sato¹, Yuta Fujiwara¹, and Akihito Sano¹

Abstract—We have been developing human-sized biped robots based on passive dynamic mechanisms. In human locomotion, the muscles activate at the same rate relative to the gait cycle during running. To achieve adaptive running for robots, such characteristics should be reproduced to yield the desired effect. In this study, we designed a central pattern generator (CPG) involving fast and slow adaptation to achieve human-like running using a simple spring-mass model and our developed bipedal robot, which is equipped with actuators that imitate the human musculoskeletal system. Our results demonstrate that fast and slow adaptations can reproduce human-like running with a constant rate of muscle firing relative to the gait cycle. Furthermore, the results suggest that the CPG contributes to the adjustment of the muscle activation timing in human running.

I. INTRODUCTION

We have been developing human-sized bipedal robots based on passive dynamic mechanisms. McGeer [1] developed a simple bipedal robot with passive legs attached to the hip; this robot could walk stably without the need for any energy input other than gravity by descending a slope. The aforementioned study indicated that passive locomotion can play a significant role in gait, and several researchers have investigated gait mechanisms using simple models [2]–[6]. In this perspective, the spring-loaded inverted pendulum (SLIP) model, comprising a point mass and prismatic massless spring, can effectively reproduce the dynamics of running [7]–[11]. To realize the running motion, we developed a bipedal robot that utilizes bouncing rod dynamics [12]. Recently, we developed a bipedal robot with actuators that could imitate the human musculoskeletal system, while utilizing the passive nature of the dynamics of the robot [13].

Walking and running locomotion is executed through dynamic interactions between the nervous system, body, and environment. Accordingly, bipedal robot controllers have been proposed based on human neurophysiology. Reportedly, the centers involved in the execution of patterned locomotion in humans, such as walking and running, exist at the lower levels of the central nervous system (e.g., the spinal cord and brainstem), which are simulated via central pattern generators (CPGs) [14]–[17]. CPGs employ a hierarchical network of rhythm generators that generate the rhythm of walking and running and pattern formulators, which are responsible

for the timing of muscle activation. Several researchers have investigated the emergence of gait through the interaction of CPGs, which are assigned to legs [18]–[22]. Aoi and Tsuchiya [23], [24] reported that stable walking can be achieved in a bipedal compass model by adaptively changing the gait period using a CPG that involves phase resetting, which is inspired by the rhythm resetting of human walking.

Observably, humans fire their muscles at the same rate relative to the gait cycle during running [25]. Thus, to achieve adaptive running using robots, such a characteristic should be reproduced. When a CPG is used solely with phase resetting for running control, although the overall period can be adaptively varied, adjusting the timing of muscle firing is unachievable as yet. Moreover, Fujiki et al. [26] report that applying slow adaptation to CPG in addition to phase resetting for controlling a compact bipedal robot walking on a split-belt, with different velocities of the left and right limbs, the motion converges to a steady-state gait.

This study proposes an adaptive control system, which is based on the current knowledge of human neurophysiology, to achieve a stable running condition in a human-sized bipedal robot. We aimed to achieve adaptive running of the bipedal robot by adjusting the actuation timings via fast and slow adaptations. We designed a CPG to manifest adaptive behavior by providing fast and slow adaptations. Specifically, in the rhythm generator, the phase angular velocity is adjusted via fast adaptation (phase resetting) and slow adaptation to the actual gait cycle. Furthermore, the pattern formulator adjusts the muscle activation timing on the basis of the leg-state feedback to yield a running pattern. We validated the proposed control system through numerical simulations of a simple running model and experiments on a bipedal robot.

II. METHOD

In this study, we propose a control system based on a CPG to achieve adaptive actuation timings using fast and slow adaptation mechanisms. We designed a rhythm generator that adapted to the gait cycle, which was determined by the interaction between the robot body and environment, and a pattern formulator that controlled the actuators based on the rhythm generator.

A. Bipedal robot based on passive dynamics

The human-sized bipedal robot, developed in our laboratory, is illustrated in Fig. 1 (leg length: 0.76 [m]; body mass: 20 [kg]). The robot is composed of passive elements such

¹Yusuke Sakurai, Tomoya Kamimura, Yuki Sakamoto, Shohei Nishii, Kodai Sato, Yuta Fujiwara, and Akihito Sano are with Department of Electrical and Mechanical Engineering, Nagoya Institute of Technology, Aichi, Japan kamimura.tomoya@nitech.ac.jp

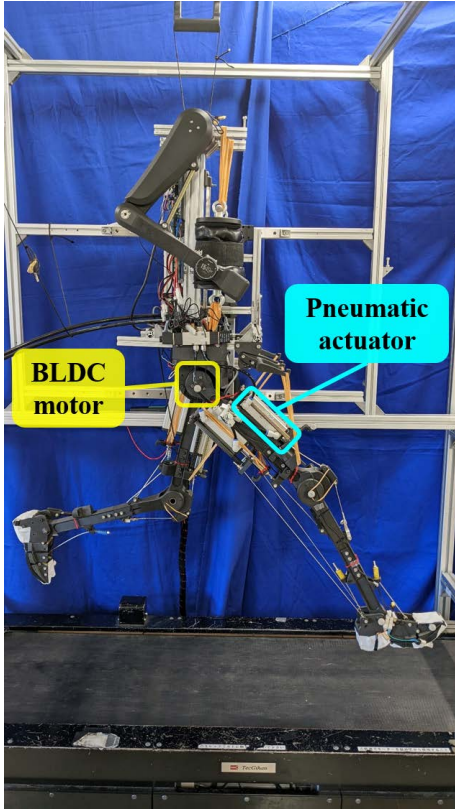


Fig. 1. Bipedal running robot. BLDC motors in hip joints actuate thigh links. Muscle-tendon system represented by pneumatic actuators actuates knee and foot links.

as springs and rubber bands. However, a minimum number of actuators are implemented because the energy input is a prerequisite for running on flat ground. In particular, the vastus muscles, which are involved in knee extension, are represented by a wire connected to a pneumatic actuator (CDQ2A63-75DZ, AirTAC). In addition, a brushless direct current (BLDC) motor (RMD-X8 Pro, MyActuator) is used to actuate the hip-joint extension. To assist in thigh extension, a rubber band is connected between the pelvis and thigh to act as the thigh muscle. The touchdown timings are sensed using a pressure sensor (FSR406, Interlink Electronics) on the sole.

B. Rhythm generator with fast and slow adaptations

We designed a rhythm generator involving fast and slow adaptations to adjust its cycle period to the actual gait cycle. Moreover, this strategy guaranteed that the left and right legs move in opposite phases. The rhythm generator was constructed as coupled oscillators of the left and right legs, where the phase oscillators ϕ_L and ϕ_R were defined for each leg. We defined the n th half-period (the time from the landing of one leg till the landing of the other leg) as T_n , and the half-period estimated by the phase oscillator as T_n^e . The basic angular velocity of the phase oscillator was defined as π/T_n^e . As explained later, we designed the rhythm generator with slow adaptation to allow the estimated period T_n^e to converge to the actual period T_n , which was

determined by the interaction between the body and the environment. Because the left and right legs are designed to move in opposite phases, the target value of the left-right phase difference is π . Furthermore, to adapt the oscillator period to the gait cycle immediately, we introduced phase resetting [14] at the moment of touchdown. Based on the design of the phase oscillator proposed by Aoi et al. [24], the dynamics of each phase oscillator were determined as follows:

$$\dot{\phi}_R = \frac{\pi}{T_n^e} + \varepsilon \sin\{(\phi_L - \phi_R) - \pi\} - \phi_R^{\text{td}} \delta(t - t_R^{\text{td}}), \quad (1a)$$

$$\dot{\phi}_L = \frac{\pi}{T_n^e} + \varepsilon \sin\{(\phi_R - \phi_L) - \pi\} - \phi_L^{\text{td}} \delta(t - t_L^{\text{td}}), \quad (1b)$$

where ε denotes the gain of the phase difference, ϕ_L^{td} and ϕ_R^{td} represent the phases of the left and right oscillators at the touchdown moment, respectively, and t_L^{td} and t_R^{td} symbolize the moments when the touchdown occurs. The third term of each oscillator indicates the fast adaptation (phase reset) at the touchdown moment. The estimated half-period T_n^e is designed to converge to the actual half-period T_n by the following update rule as a slow adaptation by using the gain K_p , K_d , and the periodic difference $\Delta T_n = T_n^e - T_n$ as

$$T_{n+1}^e = T_n^e - K_p \Delta T_n - K_d \frac{\Delta T_n - \Delta T_{n-1}}{T_n}. \quad (2)$$

We defined the phase difference $\phi = \phi_R - \phi_L$ and phase sum $\psi = \phi_R + \phi_L$. Using (1), we obtained

$$\dot{\phi} = 2\varepsilon \sin \phi - \phi_R^{\text{td}} \delta(t - t_R^{\text{td}}) + \phi_L^{\text{td}} \delta(t - t_L^{\text{td}}), \quad (3a)$$

$$\dot{\psi} = \frac{2\pi}{T_n^e} - \phi_R^{\text{td}} \delta(t - t_R^{\text{td}}) - \phi_L^{\text{td}} \delta(t - t_L^{\text{td}}). \quad (3b)$$

From (3), we further obtained

$$\phi_{n+1}^- = 2 \tan^{-1} \left\{ e^{2\varepsilon T_n} \tan \left(\frac{\phi_n^+}{2} \right) \right\}, \quad (4a)$$

$$\psi_{n+1}^- = \psi_n^+ + \frac{2\pi T_n}{T_n^e}, \quad (4b)$$

$$\phi_n^+ = \frac{(-1)^n \psi_n^- + \phi_n^-}{2}, \quad (4c)$$

$$\psi_n^+ = \frac{\psi_n^- + (-1)^n \phi_n^-}{2}, \quad (4d)$$

where ϕ_n^- and ψ_n^+ indicate the phases immediately before and after the n th touchdown, respectively. We assumed that running was initiated upon touchdown of the right leg in our experiment. Therefore, an odd number of n indicates the touchdown of the right leg, and an even number of n indicates the touchdown of the left leg.

C. Pattern formulator for reproducing human-like actuation timing

To achieve human-like running, we designed a pattern formulator, which was based on the muscle activity during human running [25]. Based on the phase angles of the rhythm generator, the pattern formulator switches the control laws of the hip and vastus pneumatic actuators.

The phases are categorized into three ranges, as illustrated

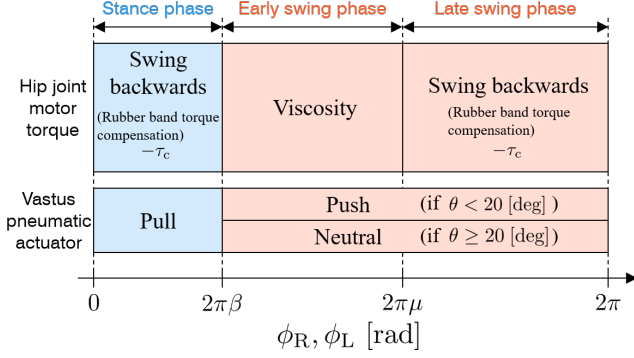


Fig. 2. Phases of rhythm generator are categorized into three phases: stance, early swing, and late swing. Pattern formulator switches control laws of actuators (hip joint motor and vastus pneumatic actuator) according to phase angle ϕ_i ($i = L, R$).

in Fig. 2. The stance phase is defined as the phase range $0 \leq \phi_i < 2\pi\beta$ ($i = L, R$), and the swing phase is defined as the phase range $2\pi\beta \leq \phi_i < 2\pi$, where β indicates the duty rate, which is determined using measured human data [25]. Furthermore, we categorized the stance phase into two phases: the early swing phase ($2\pi\beta \leq \phi_i < 2\pi\mu_n$) and the late swing phase ($2\pi\mu_n \leq \phi_i < 2\pi$), where the rate μ_n is defined hereafter.

The output torque of the hip motor is switched according to the phase. In the stance phase, the leg exerts a force (i.e. kicks) on the ground because the motor outputs a constant torque τ_c while compensating for the torque generated by the rubber bands. During the early swing phase, a rubber band is used to swing the leg forward. In the late swing phase, the motor outputs a torque τ_c to retract the legs.

The pneumatic actuator switches the output according to the phase and state of the leg. The thigh angle θ is defined as the current angle with respect to the vertical downward direction of the robot, where the swing-forward direction is positive. During the stance phase, the pneumatic actuator tightens the vastus muscle wire. When the stance phase of the rhythm generator terminates or the leg is lifted off the ground, the pneumatic actuator relaxes the vastus muscle wires to prevent the robot from hitting the ground. When the thigh angle θ exceeded a specific angle (we used 20 [deg] in the experiments), the vastus muscle wire was slightly tightened in preparation for the subsequent landing.

To maintain a steady running movement, a constant thigh-swing angle must be maintained regardless of the gait cycle. To achieve this condition, we introduced slow adaptation into the pattern formulator. Specifically, adjusting the rate μ_n appropriately using the feedback of the thigh swing angle is a prerequisite for properly adjusting the time between touchdown and the beginning of the late swing phase. To follow the target angle θ_d^s , we measured the thigh angle θ_n^s at the beginning of the late swing phase and calculated μ_{n+1}

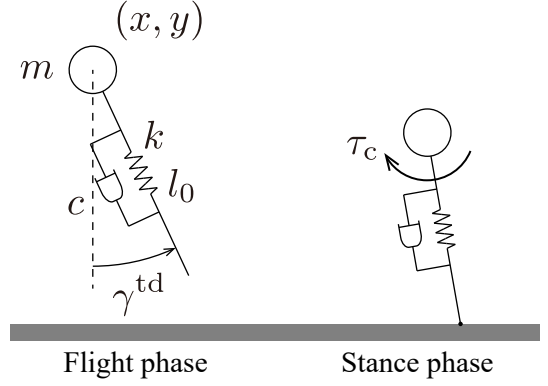


Fig. 3. Simple SLIP model with leg damper and hip actuator.

by using the gain K_μ as follows:

$$\mu_{n+1} = \mu_n - K_\mu(\theta_n^s - \theta_d^s). \quad (5)$$

III. SIMPLE MODEL SIMULATION

Before real robot experiments, we conducted numerical simulations to confirm the validity of our controller, especially focusing on the slow adaptation of the estimated half-period expressed by (2) using a simple running model. We used a spring-loaded inverted pendulum (SLIP) model, which consists of a point mass m and a massless leg (Fig. 3). The leg is represented by a prismatic spring k and damper c . The horizontal and vertical positions of the mass are represented by x and y , respectively. The gravitational acceleration is g . When the leg is in the air, its length remains l_0 and its angle keeps the touchdown angle γ^{td} . When the tip of the leg reaches the ground, it is constrained on the ground and behaves as a frictionless joint. When the stance leg returns to its nominal length after compression, the tip leaves the ground, and the leg angle immediately returns to the touchdown angle. In the stance phase, the leg is actuated by the hip motor constant torque τ_c . The equation of motion is given by

$$M(\mathbf{q})\ddot{\mathbf{q}} + H(\mathbf{q}, \dot{\mathbf{q}}) + G(\mathbf{q}) = \mathbf{T}, \quad (6)$$

where $\mathbf{q} = [x, y]^T$. $M(\mathbf{q})$, $H(\mathbf{q}, \dot{\mathbf{q}})$, $G(\mathbf{q})$, and \mathbf{T} represent inertia matrix, Coriolis and centrifugal forces, conservative forces, and actuator input, respectively. According to human parameter [27], we set $m = 50$ [kg], $l_0 = 1$ [m], $k = 8000$ [N/m], $c = 20$ [Ns/m], and $g = 9.8$ [m/s²]. Furthermore, we heuristically set $\varepsilon = 8$, $\beta = 0.1$, $\tau_c = 50$ [Nm], and $\gamma^{td} = \pi/6$ [rad]. Because our model involves a massless leg, control torque terms related to leg inertia (Fig. 2) are omitted in the simulation. When the step number is odd, the right leg CPG controls the leg, and when it is even, the left CPG controls the leg.

The simulation results for $(K_p, K_d) = (0, 0)$ (without feedback) and $(K_p, K_d) = (0.5, 0.2)$ (with feedback) are shown in Fig. 4. For both cases, at first, state variables seem to be converged to certain periodic motions. However, although the model fell down in 33 steps without feedback,

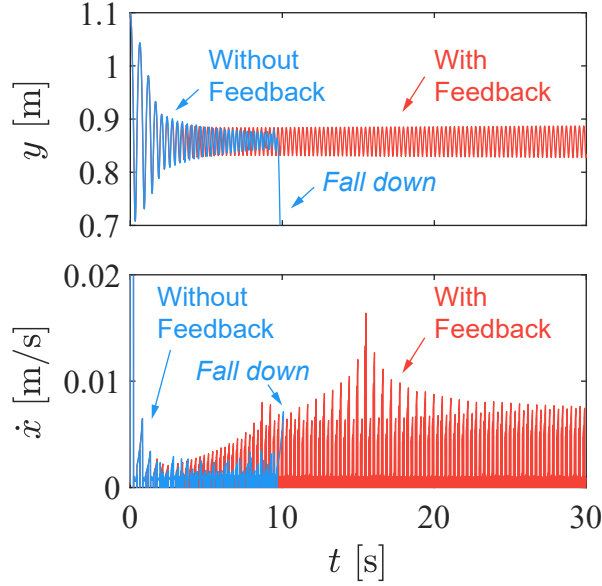


Fig. 4. Time profiles of y and \dot{x} of SLIP model. Blue and red lines indicate results for $(K_p, K_d) = (0, 0)$ (without feedback) and $(0.5, 0.2)$ (with feedback), respectively. Model falls down around 10 [s] without feedback.

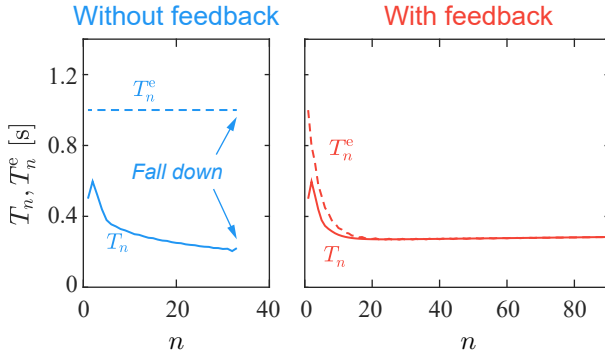


Fig. 5. Response of T_n (solid line) and T_n^e (dashed line) to step number n for $(K_p, K_d) = (0, 0)$ (without feedback) and $(0.5, 0.2)$ (with feedback), respectively.

it run over 80 steps with feedback.

The simulation results of step duration are shown in Fig. 5, where the initial estimated value is set as $T_0^e = 1$ [s]. Although T_n^e was not adjusted in the case without feedback, T_n and T_n^e asymptotically approached and converged to each other in the case with feedback.

Fig. 6 presents the response of ϕ_N^- and ψ_N^- to N , where $n = 2N - 1$. Herein, we used the stride number N instead of the step number n to focus solely on the touchdown moments of the right leg. Notably, the stride refers to the footfall number focusing only on the right leg. Although ϕ_N^- and ψ_N^- did not converge in the case without feedback, they converged to π and 3π , respectively, in the case with feedback. Therefore, by adjusting T_n^e using slow adaptation, the phase difference approaches the opposite phase π and the phase sum approaches 3π as N increases, indicating that the phase has been adjusted to increase by exactly 2π during

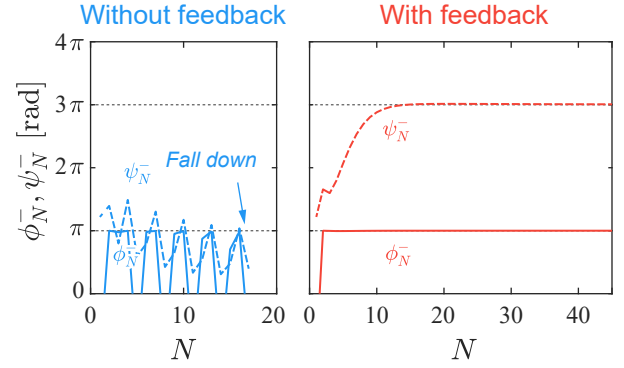


Fig. 6. Responses of phase difference ϕ_N^- (solid line) and phase sum ψ_N^- (dashed line) to stride number N for $(K_p, K_d) = (0, 0)$ (without feedback) and $(K_p, K_d) = (0.5, 0.2)$ (with feedback), respectively.

one cycle.

The aforementioned results demonstrate that the estimated half-period T_n^e can be adapted to the actual period via slow adaptation while guaranteeing the left-right opposite phase. Therefore, even if there remains a mismatch between the actual period and the initial value of the estimated half-period, muscle activation can be effectively performed at the same timing like humans using the slow adaptation.

IV. ROBOT EXPERIMENT

A. Fast and slow adaptation of estimated gait cycle

To verify the effect of fast and slow adaptation of the estimated half-period, we performed experiments on the robot for $K_p = 0$ and 0.1 in (2), respectively. For simplicity, we set $K_d = 0$ in the experiments. In these experiments, we assumed the absence of a feedback of the thigh angle in the pattern formulator, which was achieved by setting $\mu_n = \mu = \text{const.}$ For the rhythm generator, we set $\varepsilon = 4$ and $T_0^e = 550$ [ms]. The value of ε was set based on some preliminary experiments. When ε is set too small, the convergence of the relative phase ϕ is too slow, causing the robot's left and right legs to be unable to move alternately, ultimately leading to a fall.

For the pattern formulator, based on human parameter and several preliminary experiments, we set $\beta = 0.25$, $\mu = 0.6$, and $\tau_c = 3$ [Nm]. Note that the duty rate in human running is about 35 % and the hip extensor muscle groups begin to contract after 50 % of the gait cycle [25]. The treadmill speed during the experiment was set at 10 [km/h]. The robot is constrained in the sagittal plane. The operator can assist by pulling the robot up from above.

Fig. 7 presents a plot of the response of the estimated half-period T_n^e to the number of steps n . For $K_p = 0$, T_n^e maintained its initial value of 550 [ms], regardless of the actual half-period T_n because the estimated half-period was not adjusted. In contrast, for $K_p = 0.1$, the estimated half-period T_n^e and actual half-period T_n asymptotically converge to each other, as shown in the simple model simulation (Fig. 5). Furthermore, in both experiments, the fast adaptation enabled

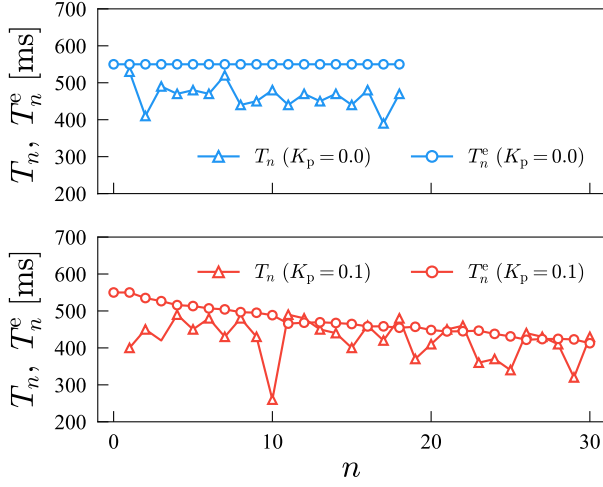


Fig. 7. Responses of actual and estimated half-period T_n (triangle) and T_n^e (circle) to n . Blue and red lines indicate $K_p = 0$ (top) and $K_p = 0.1$ (bottom), respectively.

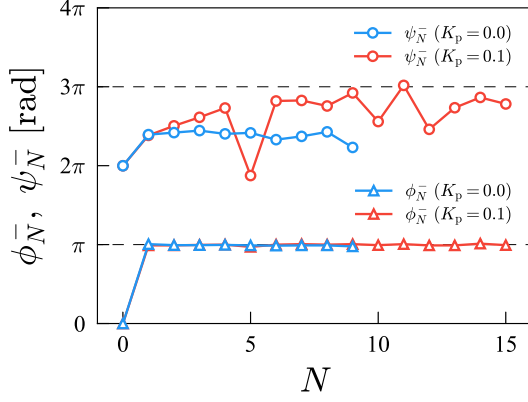


Fig. 8. Responses of phase difference ϕ_N^- (triangle) and phase sum ψ_N^- (circle) at touchdown moments of right leg to N . Blue and red lines indicate $K_p = 0$ and $K_p = 0.1$, respectively. Horizontal lines indicate π and 3π , respectively.

running, even when there remained a mismatch between T_n^e and T_n .

Fig. 8 depicts the change of phase difference ϕ_N^- and phase sum ψ_N^- at the moment immediately prior to the touchdown of the right leg with respect to N . For both $K_p = 0$ and 0.1 , the phase difference ϕ_N^- converges to π . On the other hand, while ψ_N^- remained at approximately 2.5π for $K_p = 0$, it increased to approximately 3π for $K_p = 0.1$.

Although the robot achieved sustained running until $N = 15$, it could not achieve steady running and fell after running. This fall was a result of a stumble caused by the gradually decreasing thigh-swing angle. The response of thigh angle θ_N^- to N is plotted in Fig. 9. The swing angle of the thigh gradually decreases as N increases.

B. Slow adaptation of pattern formulator

Furthermore, we verified that a longer period of sustained running can be achieved without operator assistance by adjusting μ_n on the basis of the thigh-angle feedback in

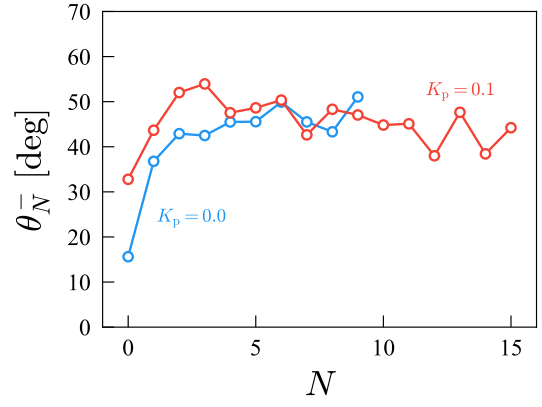


Fig. 9. Response of swing angle of thigh θ_N^- at touchdown moments of right leg to N . Blue and red lines indicate $K_p = 0$ and $K_p = 0.1$, respectively.

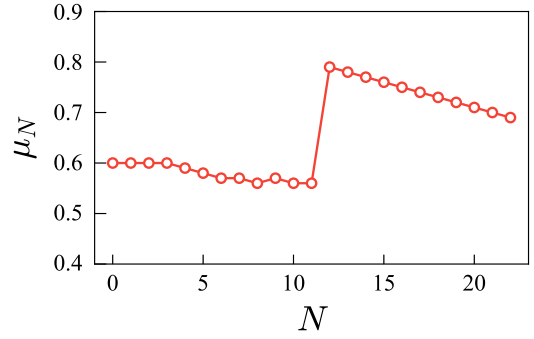


Fig. 10. Response of adaptive μ_N to N .

the pattern formulator. μ_n was determined using (5). In accordance with the relationship between the actual swing angle θ_n^s and target swing angle θ_d^s , the value of K_μ is switched as follows:

$$K_\mu = \begin{cases} 0.005, & (\theta_n^s > \theta_d^s) \\ 20 \times 0.005, & (\theta_n^s \leq \theta_d^s) \end{cases} \quad (7)$$

This condition yields a strong adjustment when the thigh-swing angle θ_n is smaller than the target value θ_d . In the experiment, we set $\theta_d^s = 35$ [deg] based on the human running and $K_p = 0.1$. Note that in human running [25], the hip joint switches from extension to flexion when the leg angle to the vertical direction is about 32 [deg].

Fig. 10 presents the response of μ_N to N . μ_N decreases and converges to approximately 0.55 around $N = 6$ to 12. When $N = 12$, μ_N increases substantially to an approximate value of 0.80 and subsequently decreases again.

The response of T_n^e to n is plotted in Fig. 11. When μ_n is adaptive, the decrement rate of T_n^e is suppressed, and T_n^e converges to a constant value (≈ 440 [ms]) as n increases.

Fig. 12 presents the plot of the right-thigh angle θ_N^- with respect to N . The swing angle decreases regardless of the value of μ_N until $N = 9$. In contrast, after $N = 10$, although the swing angle continues to decrease when μ_N is constant, it increases with N when μ_N is adaptive.

The obtained results reveal that the adaptive μ_n prevents

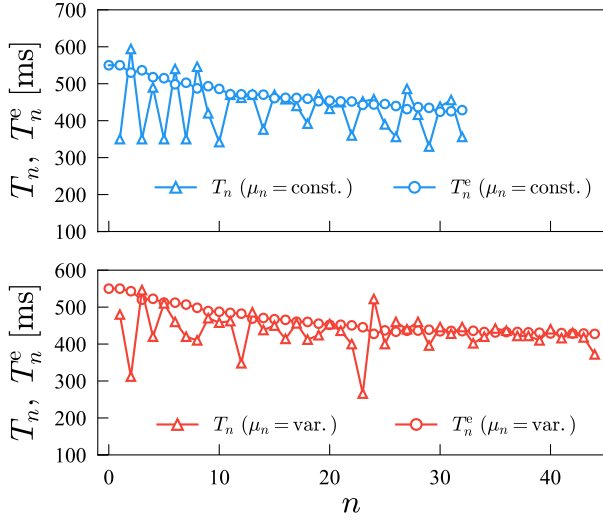


Fig. 11. Response of T_n (triangle) and T_n^e (circle) to n . Blue and red lines indicate results using constant (top) and adaptive (bottom) μ_n , respectively.

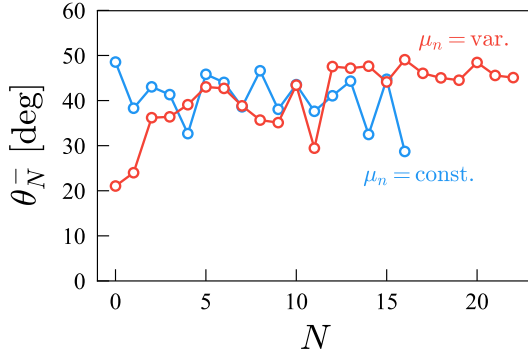


Fig. 12. Response of thigh swing angle θ_N^- to N . Blue and red lines indicate results using constant and adaptive μ_n , respectively.

the monotonic decrease in the thigh swing angle, thereby resulting in continuous running of more than $N = 20$.

V. DISCUSSION

A. Effect of estimated gait cycle adaptation

In this study, to realize a bipedal robot capable of running with human-like actuation timing, we designed a controller based on the CPG that could adapt its gait cycle through slow adaptation, in addition to fast adaptation (phase resetting). Notably, the results validated that both the simple model and the robot could achieve continuous running. Moreover, owing to the slow adaptation of the rhythm generator, the estimated gait cycle and the actual gait cycle asymptotically approached each other through slow adaptation (Figs. 5 and 7), whereas the left and right legs were moved in opposite phases by employing the phase-difference compensation term. Furthermore, fast adaptation allowed the robot to run even for a mismatch between the estimated and actual gait cycles. These results suggest that the fast and slow adaptation of the rhythm generator plays an significant role to generate the adaptive locomotion. In the real robot experiment, the pattern

formulator actuated the pneumatic actuators, which represent the vastus muscles of the robot, and the BLDC motors, which represent the hip extensor muscle groups, according to the phase angle of the rhythm generator. Therefore, the obtained results demonstrated that the robot could reproduce human-like running with a constant rate of muscle firing relative to the gait cycle, regardless of the actual running cycle, owing to the fast and slow adaptation of the rhythm generator.

However, when we solely utilized adaptation in the rhythm generator, the running motion could not be sustained for a long time. The thigh-swing angle decreased as the number of steps increased, thereby leading to this inability, as illustrated in Fig. 9. In particular, this result was presumably a result of the constant μ_n used in the pattern formulator. When the initial value of the estimated half-period T_n^e is larger than the actual half-period T_n , T_n^e decreased as n increased owing to slow adaptation, where the phase angular velocity of the rhythm generator increased. This resulted in a short stance phase, and the robot could not kick the ground sufficiently. Moreover, the swing angle also decreased because the duration of the early swing phase was reduced. In particular, the repetition of such a sequence is expected to decrease the swing angle of the thighs. This experimental result suggested that a further adaptation mechanism is required to achieve continuous running.

B. Effect of μ_n adaptation

We achieved the continuous running of our bipedal robot for approximately $N = 20$ by adjusting μ_n in the pattern formulator. The robot's fall was prevented by adjusting μ_n appropriately when the thigh swing angle temporarily decreased to an inappropriate value, as shown in Fig. 12, thereby yielding the successful result. Furthermore, μ_n converged to a certain value of approximately 0.55 for $N = 6$ to 11, as depicted in Fig. 10. This result suggests the existence of an appropriate μ_n for running, generated by the dynamic interaction between the body of the robot and the environment. Therefore, the obtained results suggest that humans invariably activate their muscles at the same rate with respect to the gait cycle using the appropriate muscle activation timing, which is defined by the dynamic interaction between the human body and the environment.

However, even when we used the pattern formulator with slow adaptation, the robot could not maintain continuous running for a long period. We discovered that the thigh angle at liftoff timing gradually decreased during running, thereby causing difficulties for the robot to kick the ground. This trend resulted in the robot's inability to lift itself upward sufficiently, and the robot consequently stumbled and fell onto the treadmill. As indicated by the results in Fig. 12, θ_N^- was maintained at approximately 50 [deg] after $N = 12$, following the considerable change in μ_N . To achieve longer periods of continuous running, the duty rate β in the pattern formulator should be accordingly adjusted, which will result in an appropriate swing angle.

VI. CONCLUSION

In this study, we designed a CPG involving fast and slow adaptation and a constant muscle activation timing to achieve human-like running motion of a bipedal robot.

Consequently, the CPG adapted to the actual period and achieved continuous running for both the simple model and the actual bipedal robot. Furthermore, the results suggested that the CPG contributed to adjusting the muscle firing timing properly according to the state of the body, which could also result in optimum timing for human running.

However, in the robot experiment, even upon the implementation of the CPG with fast and slow adaptation, the swing angle of the thigh decreased as the number of steps increased, and the robot was unable to achieve continuous running for a long period. In future research, we will adjust the duty ratio β on the basis of the swing angle.

Moreover, we will aim to improve upon the developed running robot and develop a walking robot to elucidate its relationship to adaptive human locomotion. Thus, further studies in this research direction will lead to engineering applications not only for improved bipedal robots but also for walking assistive devices.

ACKNOWLEDGEMENT

This work was supported in part by JSPS KAKENHI Grant Number JP21K14104 and JP22H01445.

REFERENCES

- [1] T. McGeer, "Passive dynamic walking," *The International Journal of Robotics Research*, vol. 9, pp. 62–82, 1990.
- [2] M. Garcia, A. Chatterjee, A. Ruina, and M. Coleman, "The simplest walking model: stability, complexity, and scaling," *Journal of Biomechanical Engineering*, vol. 120, pp. 281–288, 1998.
- [3] A. Goswami, B. Thuilot, and B. Espiau, "A study of the passive gait of a compass-like biped robot: Symmetry and chaos," *International Journal of Robotics Research*, vol. 17, pp. 1282–1301, 1998.
- [4] S. Collins, A. Ruina, R. Tedrake, and M. Wisse, "Efficient bipedal robots based on passive-dynamic walkers," *Science*, vol. 307, pp. 1082–1085, 2005.
- [5] Y. Ikemata, K. Yasuhara, A. Sano, and H. Fujimoto, "A study of the leg-swing motion of passive walking," *Proceedings - IEEE International Conference on Robotics and Automation*, pp. 1588–1593, 2008.
- [6] K. Okamoto, S. Aoi, I. Obayashi, H. Kokubu, K. Senda, and K. Tsuchiya, "Disappearance of chaotic attractor of passive dynamic walking by stretch-bending deformation in basin of attraction," in *2020 IEEE/RSJ International Conference on Intelligent Robots and Systems (IROS)*, 2020.
- [7] R. Blickhan, "The spring-mass model for running and hopping," *Journal of Biomechanics*, vol. 22, pp. 1217–1227, 1989.
- [8] R. Full and D. Koditschek, "Templates and anchors: neuromechanical hypotheses of legged locomotion on land," *The Journal of Experimental Biology*, vol. 202, pp. 3325–3332, 1999.
- [9] H. Geyer, A. Seyfarth, and R. Blickhan, "Spring-mass running: Simple approximate solution and application to gait stability," *Journal of Theoretical Biology*, vol. 232, pp. 315–328, 2005.
- [10] K. Clark and P. Weyand, "Are running speeds maximized with simple-spring stance mechanics?" *Journal of Applied Physiology*, vol. 117, pp. 604–615, 2014.
- [11] Z. Gan, Y. Yesilevskiy, P. Zaytsev, and C. D. Remy, "All common bipedal gaits emerge from a single passive model," *Journal of the Royal Society Interface*, vol. 15, 2018.
- [12] H. Miyamoto, A. Sano, Y. Ikemata, S. Maruyama, and H. Fujimoto, "A study of bouncing rod dynamics aiming at passive running," in *IEEE International Conference on Robotics and Automation, ICRA2010*, IEEE, 2010, pp. 3298–3303.
- [13] T. Kamimura, K. Sato, D. Murayama, N. Kawase, and A. Sano, "Dynamical effect of elastically supported wobbling mass on biped running," in *IEEE/RSJ International Conference on Intelligent Robots and Systems, IROS2021*, 2021, pp. 4048–4055.
- [14] I. A. Rybak, N. A. Shevtsova, M. Lafreniere-Roula, and D. A. McCrear, "Modelling spinal circuitry involved in locomotor pattern generation: Insights from deletions during fictive locomotion," *Journal of Physiology*, vol. 577, pp. 617–639, 2006.
- [15] G. Cappellini, Y. P. Ivanenko, R. E. Poppele, and F. Lacquaniti, "Motor patterns in human walking and running," *Journal of Neurophysiology*, vol. 95, pp. 3426–3437, 2006.
- [16] Y. P. Ivanenko, G. Cappellini, N. Dominici, R. E. Poppele, and F. Lacquaniti, "Modular control of limb movements during human locomotion," *Journal of Neuroscience*, vol. 27, pp. 11 149–11 161, 2007.
- [17] Y. I. Molokov, B. J. Bacak, A. E. Talpalar, and I. A. Rybak, "Mechanisms of left-right coordination in mammalian locomotor pattern generation circuits: A mathematical modeling view," *PLoS Computational Biology*, vol. 11, no. 5, e1004270, 2015.
- [18] G. Taga, Y. Yamaguchi, and H. Shimizu, "Self-organized control of bipedal locomotion by neural oscillators in unpredictable environment," *Biological Cybernetics*, vol. 65, pp. 147–159, 1991.
- [19] P. Manoonpong and F. Wörgötter, "Efference copies in neural control of dynamic biped walking," *Robotics and Autonomous Systems*, vol. 57, pp. 1140–1153, 2009.
- [20] Y. Fukuoka, Y. Habu, and T. Fukui, "Analysis of the gait generation principle by a simulated quadruped model with a cpg incorporating vestibular modulation," *Biological Cybernetics*, vol. 107, pp. 695–710, 2013.
- [21] S. Aoi, P. Manoonpong, Y. Ambe, F. Matsuno, and F. Wörgötter, "Adaptive control strategies for interlimb coordination in legged robots: A review," *Frontiers in Neurorobotics*, vol. 11, pp. 1–21, 2017.
- [22] S. Fujiki, S. Aoi, T. Funato, Y. Sato, K. Tsuchiya, and D. Yanagihara, "Adaptive hindlimb split-belt treadmill walking in rats by controlling basic muscle activation patterns via phase resetting," *Scientific Reports*, vol. 8, 17341, 2018.
- [23] S. Aoi and K. Tsuchiya, "Bifurcation and chaos of a simple walking model driven by a rhythmic signal shinya," *International Journal of Non-Linear Mechanics*, vol. 41, pp. 438–446, 2006.
- [24] S. Aoi and K. Tsuchiya, "Self-stability of a simple walking model driven by a rhythmic signal," *Nonlinear Dynamics*, vol. 48, pp. 1–16, 2007.
- [25] J. B. J. Perry, *Gait analysis: Normal and pathological function, Second edition*. Slack Incorporated, New Jersey, 2010.
- [26] S. Fujiki, S. Aoi, T. Funato, N. Tomita, K. Senda, and K. Tsuchiya, "Adaptation mechanism of interlimb coordination in human split-belt treadmill walking through learning of foot contact timing: A robotics study," *Journal of the Royal Society Interface*, vol. 12, 20150542, 2015.
- [27] H. Geyer, A. Seyfarth, and R. Blickhan, "Compliant leg behaviour explains basic dynamics of walking and running," *Proceedings of the Royal Society B: Biological Sciences*, vol. 273, pp. 2861–2867, 2006.